Contents lists available at ScienceDirect

Biomedicine & Pharmacotherapy

journal homepage: www.elsevier.com/locate/biopha

Liver-targeted nanoparticles delivering nitric oxide reduce portal hypertension in cirrhotic rats

Meritxell Perramón [a,b,*], María Navalón-López [c], Guillermo Fernández-Varo [a,b], Alazne Moreno-Lanceta [a,f], Rocío García-Pérez [d], Joana Faneca [a], Mario López-Moya [c], Cristina Fornaguera [c], Judith García-Villoria [a,e], Manuel Morales-Ruiz [a,b,f], Pedro Melgar-Lesmes [a,b,f,g], Salvador Borrós [c], Wladimiro Jiménez [a,b,f]

[a] Biochemistry and Molecular Genetics Service, Hospital Clínic of Barcelona, Institut d'Investigacions Biomèdiques August Pi i Sunyer (IDIBAPS), Barcelona, Spain
[b] Centro de Investigación Biomédica en Red de Enfermedades Hepáticas y Digestivas (CIBERehd), Madrid, Spain
[c] Grup d'Enginyeria de Materials (Gemat), Institut Químic de Sarrià (IQS), Universitat Ramon Llull (URL), Barcelona, Spain
[d] Hepatopancreatobiliary Surgery & Transplantation, General & Digestive Surgery Service, Digestive & Metabolic Disease Institute (ICMDM) of Hospital Clínic of Barcelona, Barcelona, Spain. Department of Medicine, University of Barcelona, Barcelona, Spain
[e] Centro de Investigación Biomédica en Red de Enfermedades Raras (CIBERER), Madrid, Spain
[f] Department of Biomedicine, University of Barcelona, Barcelona, Spain
[g] Institute for Medical Engineering and Science, Massachusetts Institute of Technology, Cambridge, USA

ARTICLE INFO

ABSTRACT

Nitric oxide (NO) is a small vasodilator playing a key role in the pathogenesis of portal hypertension. Here, we assessed the potential therapeutic effect of a NO donor targeted to the liver by poly(beta-amino ester) nanoparticles (pBAE NPs) in experimental cirrhosis. Retinol-functionalized NO donor pBAE NPs (Ret pBAE NPs) were synthetized with the aim of actively targeting the liver. Administration of Ret pBAE NPs resulted in uptake and transfection by the liver and spleen. NPs were not found in other organs or the systemic circulation. Treatment with NO donor Ret pBAE NPs (30 mg/ kg body weight) significantly decreased aspartate aminotransferase, lactate dehydrogenase and portal pressure (9.75 ± 0.64 mmHg) compared to control NPs (13.4 ± 0.53 mmHg) in cirrhotic rats. There were no effects on mean arterial pressure and cardiac output. Liver-targeted NO donor NPs reduced collagen fibers and steatosis, activation of hepatic stellate cells and mRNA expression of profibrogenic and proinflammatory genes. Finally, Ret pBAE NPs displayed efficient transfection in human liver slices. Overall, liver-specific NO donor NPs effectively target the liver and mitigated inflammation and portal hypertension in cirrhotic rats. The use of Ret pBAE may prove to be an effective therapeutic strategy to treat advanced liver disease.

1. Introduction

Portal hypertension is a characteristic syndrome of patients with advanced liver disease and develops concomitantly with systemic arterial hypotension and hyperkinetic circulation [1]. An important factor contributing to the increase in portal pressure (PP) is the elevation of intrahepatic vascular resistance [2,3]. A deficit in the intrahepatic bioavailability of the endogenous vasodilator nitric oxide (NO) has been described as one of the most relevant contributory factors involved in the pathogenesis of this phenomenon [4]. In the last years, several strategies have been proposed to improve the availability of NO in hepatic tissue. However suboptimal results were obtained with most of

these therapeutic approaches [5]. This lack of efficacy is mainly due to ineffective liver-cell targeting, and the remarkable dissimilarity in NO production by the hepatic and systemic vasculatures [6]. In contrast to what occurs in the liver circulation, the systemic vessels of cirrhotic patients are characterized by increased NO production and activity, which, in turn, lead to arteriolar vasodilation and arterial hypotension. Therefore, any non-targeted strategy attempting to deliver NO to the liver may result in an unwanted accentuation of the systemic circulatory dysfunction already present in decompensated liver disease [3,7].

The current investigation was aimed at assessing whether this problem could be overcome by selectively delivering NO to the hepatic vascular bed. Furthermore, we also hypothesized that liver function could also benefit from NO administration because of the properties of this mediator beyond its vasodilator activity, including anti-inflammatory and regenerative properties [8]. Accordingly, we developed a new liver-targeted nanoformulation combining a cationic poly (beta-amino ester) polymer (pBAE) with an NO donor (organic nitrates) incorporated into its chemical structure which, in contact with an anionic nucleic acids, electrostatically complexes into small nanometric particles. Subsequently, we evaluated whether these pBAE nanoparticles (NPs) could ameliorate portal hypertension and improve other liver function indicators, without affecting systemic hemodynamics in experimental cirrhosis.

2. Materials and methods

2.1. Synthesis of Retinol (Ret) pBAE NPs

To selectively deliver NO to the liver, organic nitrites were selected as NO releasing moieties, pBAE NPs as delivery vehicles and Ret as a targeting molecule. pBAE are a class of robust and versatile cationic polymers that are composed of ester bonds that enable different genetic material complexation and easily degradable in physiological conditions. We used a combination of two different oligopeptide end modifications, lysine-modified pBAEs (K) and histidine modified pBAEs (H). On the other hand, the addition of a targeting moiety to the polymer potentiates the efficacy given by the active principle inside the nanosystem. In the current investigation we selected Ret (Vit A) as homing device to the liver, as we demonstrated previously [9]. Ret is highly affine to retinol binding protein, a circulating protein that is efficiently taken up by the liver due to the high hepatic expression of specific receptors. Briefly, NO donor Ret pBAE NPs were formulated according to the following combinations of polymers: K Ret (5%), H (40%) and K72-NO (55%). The so-called K72-NO polymer is a nitrooxy -terminated organic acid based on C32-CK3 polymer. Control (CT) NPs were formulated with K Ret (5%), H (40%), and K (55%) lacking the K72-NO moiety. Cell uptake and transfection efficiency were evaluated by labeling the polymer with Cyanine5 (Cy5) and loading mCherry plasmid as a reporter gene, respectively. Cy5 was added (5%) to the H polymer formulation. Equal volumes of mCherry plasmid (0.5 µg/µL) were added over the polymer combination (50 µg/µL in 12.5×10^{-3} M sodium acetate buffer solution), mixed by pipetting and incubated for 30 min at room temperature. Thereafter, the mixture was precipitated in the same volume of diethyl pyrocarbonate water to form NPs, which were further added over a HEPES (20×10^{-3} M) + sucrose (4% w/w) solution. K Ret, and KH polymers were synthetized as described previously [9]. K72-NO polymer was obtained by reacting N-bromaliphatic carboxylic acid (1 eq) and AgNO3 (1.05 eq) in acetonitrile for 24 h in the dark to obtain the organic aldehyde AgBr. It was the filtered and extracted using ethyl acetate through the addition of water to the reaction and then evaporated. C32 backbone polymer was synthetized by reacting butanediol diacrylate (1eq) and 5-aminopentanol (1.08 eq) at 90 ºC for 24 h. C32 (1 eq), dicyclohexylcarbodiimide (1.05 eq) and n-nitrooxyaliphatic carboxylic acid (1 eq) and the catalyst 4-dimethylaminopyridine (0.05 eq) were reacted in tetrahydrofuran in ice for 30 min and at room temperature for the following 48 h. The product was filtered and ether was used

to purify the polymer, which was reacted with CK3 (Ontores Lts, Shangai, China) in dimethyl sulfoxide overnight. The product (K72-NO) was purified through the precipitation of a diethyl ether–acetone mixture and stored at − 20 ºC until use. All reagents were purchased from Sigma-Aldrich (Darmstadt, Germany). All polymers were characterized by proton nuclear magnetic resonance (H NMR) as follows.

Polymer Kret ^{1}H NMR (400 MHz, cdcl3) δ 4.20 – 4.03 (m, 13 H), 3.66 – 3.54 (m, 7 H), 3.26 – 3.15 (m, 4 H), 3.02 – 2.93 (m, 9 H), 2.80 – 2.70 (m, 6 H), 2.74 (s, 4 H), 2.48 – 2.37 (m, 6 H), 2.42 (s, 5 H), 2.15 (s, 88 H), 2.18 – 2.11 (m, 23 H), 1.75 – 1.66 (m, 11 H), 1.48 – 1.37 (m, 5 H), 1.30 (s, 5 H).

Polymer K ^{1}H NMR (400 MHz, dimethylsulfoxide) δ 8.86 (s, 1 H), 8.19 (d, $J = 7.7$ Hz, 1 H), 7.95 (s, 5 H), 4.34 (d, $J = 6.1$ Hz, 1 H), 4.25 (q, $J = 7.4$ Hz, 1 H), 4.13 (d, $J = 7.1$ Hz, 1 H), 4.03 (s, 7 H), 2.83 – 2.75 (m, 1 H), 2.80 – 2.69 (m, 3 H), 2.68 – 2.60 (m, 1 H), 2.54 (s, 16 H), 2.08 (s, 1 H), 1.63 (d, $J = 4.0$ Hz, 6 H), 1.57 (d, $J = 6.9$ Hz, 1 H), 1.38 (dt, $J = 17.7$, 8.0 Hz, 4 H), 1.24 (s, 5 H), 1.09 (t, $J = 7.0$ Hz, 1 H), 0.89 – 0.82 (m, 2 H).

Polymer H ^{1}H NMR (400 MHz, dimethylsulfoxide) δ 8.55 (s, 2 H), 8.47 (s, 1 H), 7.20 (d, $J = 9.1$ Hz, 1 H), 4.48 (dq, $J = 21.8$, 6.9 Hz, 1 H), 4.01 (s, 6 H), 3.38 – 3.30 (m, 1 H), 3.05 – 2.90 (m, 1 H), 2.96 (s, 1 H), 2.77 (s, 2 H), 2.72 (s, 3 H), 2.75 – 2.64 (m, 1 H), 2.50 (s, 17 H), 2.53 – 2.43 (m, 10 H), 2.04 (s, 1 H), 1.60 (s, 5 H), 1.52 (s, 4 H), 1.38 (p, $J = 6.6$ Hz, 1 H), 1.20 (d, $J = 9.3$ Hz, 5 H), 0.81 (d, $J = 6.7$ Hz, 1 H).

K72-NO ^{1}H NMR (400 MHz, CD3OD, TMS) (ppm): = 4.48 (t. –CH2-NO3), 4.33 (br, NH2-(CH2) 4-CH-), 4.12 (t, CH2-CH2-O-), 3.57 (br, NH2-CH-CH2-S-), 2.95 (br, CH2-CH2-N-, NH2-CH2-(CH2)3-CH-), 2.83 (dd, -CH2-S-CH2-), 2.67 (br, -N-CH2-CH2-C(=O)-O), 2.35 (t. HOOC-CH2-), 1,82 (m. -OOC-CH2-CH2-), 1.74 (br, -O-CH2- CH2-CH2-CH2-O), 1.51 (m. –CH2-CH2-CH2-NO3).

2.2. Ethics approval and patient consent

Studies involving animals followed the ethical guidelines stated by the "Guide for the Care and Use of Laboratory Animals" prepared by the National Academy of Sciences and published by the National Institutes of Health (8th edition 2011). The use of experimental animals was approved by the Animal Experimentation Committee of the University of Barcelona (Barcelona, Spain) with the code CEEA-391/19 (Generalitat de Cataluya, authorization number: 11111). Research using human subject samples followed the ethical guidelines of the 1975 Declaration of Helsinki and all patients included in this study provided written and signed informed consent.

Human sample use was approved by the Investigation and Ethics Committee of the Hospital Clinic with the identification number HCB/2022/1110.

2.3. Induction of experimental liver cirrhosis

Liver cirrhosis was induced as described previously [10] in a group of male Wistar rats (Charles-River, Saint Aubin les Elseuf, France) with chronic carbon tetrachloride inhalation, until at least one week after the establishment of ascites. Animals were kept under constant temperature and humidity in 12 h controlled dark/light cycle and fed ad libitum with standard pellet and water containing phenobarbital (0.3 g/L).

2.4. Biodistribution study

Two rats intravenously (i.v.) received Cy5 mCherry Ret pBAE NPs or NPs lacking Ret (0.25 mg mCherry/kg of body weight) and were euthanized by isoflurane overdose (Forane, Abbott Laboratories S.A., Madrid, Spain) 3 h after administration. Organ and arteries were fixed in 4% paraformaldehyde, embedded in Tissue Teck O.C.T (Sakura Finetek, Tokyo, Japan) and snap-frozen in isopentane. After obtaining cryosections, nuclei were stained with Vectashield Mounting Medium with 4′,6-diamidino-2-phenylindole (DAPI). A coverslip was placed on top of the specimen and photographs were taken using a Leica TCS-SPE

confocal fluorescence microscope at 40x. For anti-αSMA fluorescent staining, hepatic cryosections were hydrated with PBS and incubated in blocking buffer (3% bovine serum albumin, 5% goat serum, 0,1% Triton X-100) for 1 h at room temperature. Subsequently, the sections were incubated with a primary mouse anti-αSMA antibody (1:100 dilution, Dako) in blocking buffer at 4 °C overnight. Next, the sections were washed three times in PBS for 5 min and incubated with a secondary goat Alexa Fluor 488-conjugated anti-mouse antibody (1:500 dilution, Thermo Fisher, Waltham, MA, USA) for 1 h at room temperature and subsequently washed three times in PBS for 5 min and mounted in DAPI.

2.5. Hemodynamic study

Cirrhotic rats with ascites were anesthetized with Inactin® (50 mg/kg body weight, Sigma-Aldrich, Steinherim, Germany). The left femoral artery and vein were isolated and catheterized with a polyethylene PE-50 polyvinyl catheter. Then, the artery was connected to a transducer to measure mean arterial pressure (MAP). To monitor intraarterial temperature during cardiac output (CO) measurement, the right jugular vein was isolated, and another catheter was placed in the right atrium and a thermocouple (Columbus Instruments, Columbus, OH) was advanced through the aortic arch via the left carotid approach. CO was measured by thermodilution following the administration of a 200 μL bolus of Ringer solution (20–23ºC) into the right atrium using a spring-loaded syringe was used (Hamilton Syringe, model CR-700–200, Reno, Nevada, USA). Both MAP and CO were recorded in a multichannel system (Powerlab, ADInstruments, Dunedin, New Zealand). Following a stabilization period of approximately 30 min after surgery, basal (0 min) MAP and CO were measured. Next, the rats randomly received 30 mg/kg body weight of CT (n = 5) or NO donor mCherry Ret pBAE NPs (n = 9) through the femoral vein. MAP was continuously recorded and CO was measured every 30 min during 120 min. At the end of this period a midline abdominal incision of 2 cm was performed and the portal vein was cannulated through the ileocolic vein to measure PP. Total peripheral resistance (TPR) was estimated as MAP/CO and splanchnic perfusion pressure (SPP) as MAP minus PP. At the end of the hemodynamic study, a blood sample from the femoral artery catheter was obtained, Then, the rats were euthanized by isoflurane overdose and liver samples were collected. Biopsies were snap frozen or fixed with 10% buffered formalin for paraffin embedding.

2.6. Preparation of human precision cut liver slices (hPCLS)

To assess the ex vivo bioavailability of NO donor Ret pBAE NPs we used human liver slices obtained from liver explants of patients undergoing liver transplantation in the Hospital Clinic (Barcelona, Spain). hPCLS were prepared as described previously [11]. In brief, excess human liver was surgically obtained, and cylindrical cores were made using a 6-mm biopsy punch (Kai Medical, Seki City, Japan) and preserved in ice-cold IGL-1 preservation solution (Lissieu, France) until slicing. Krebs-Henseleit buffer was supplemented with 25 mM D-glucose (Merck, Darmstadt, Germany), 25 mM $NaHCO_3$ (Merck), and 10 mM 4-(2-hydroxyethyl) piperazine-1-ethanesulfonic acid (MP Biomedicals, Aurora, OH), saturated with carbogen (95% O_2 and 5% CO_2), and used as slicing solution. hPCLs were obtained using a Leica VT1200 S vibratome (Leica Microsystems, Nussloch, Germany). The size of the hPCLs was adjusted for the wet weight (4–5 mg) to a thickness of around 250 μm. hPCLS were incubated in William's E medium with GlutaMAX (Life Technologies, Carlsbad) 2.75 g/mL D-glucose monohydrate (Merck, Darmstadt, Germany), 50 mg/mL gentamicin (Invitrogen, Paisley, UK) was placed in 12-well plates (1.3 mL/well), preheated and oxygenized in the incubator at 37 °C with a continuous 5% CO_2– 40% O_2 supply for at least 30 min before plating the hPCLS. The hPCLS were preincubated individually for 1 h in the culture medium while being gently shaken at 90 rev/min (basal time point).

2.7. Incubation of PCLS

After preincubation, slices were changed to preheated and oxygenized fresh medium containing mCherry Ret pBAE NPs (2 μg mCherry/mL). Slices were collected for further analysis after 48 h. At least three slices were incubated for each condition. Tissue transfection was evaluated obtaining O.C.T. cryosections and staining nuclei with DAPI. Images were taken using the Leica TCS-SP8 confocal fluorescence microscope at 40x (Leica, Nussloch, Germany).

2.8. Statistical analysis

Data were analyzed using GraphPad Prism 6 (GraphPad Software Inc., San Diego, USA). The Unpaired Student *t*-test or Mann Whitney test was performed when appropriate. Results were shown as mean ± S.E. and considered significant when $p < 0.05$.

3. RESULTS

3.1. Synthesis and physicochemical characterization of NO donor Ret pBAE NPs

NO donor Ret pBAE were synthetized as represented in Fig. 1A. CT NPs had a Z-average (hydrodynamic size) of 174.8 ± 1.51 nm, polydispersity index (PDI) of 0.11 ± 0.003 and Z-potential of 38.47 ± 0.49 mV, measured by dynamic light scattering. The addition of the NO donor to the NPs increased their size to 234.2 ± 2.38 nm and their PDI to 0.21 ± 0.02, whereas the Z-potential slightly decreased to 33.37 ± 0.96 mV (Fig. 1B).

To evaluate NP uptake by human liver cells, HepG2 and LX-2 cells were treated with CT or NO donor Ret pBAE NPs. Confocal fluorescence showed effective transfection in both types of cultured human-derived cells (Fig. 1C). Moreover, the presence of the NO donor was associated with higher concentration of nitrites and nitrates in the culture medium of these cells in comparison to cells incubated with NPs lacking the NO donor (Fig. 1D).

3.2. The cirrhotic liver is the main target of Ret pBAE NPs after in vivo administration

To investigate organ biodistribution, Cy5 mCherry Ret pBAE NPs were administered i.v. to cirrhotic rats with ascites. Organ samples were collected 3 h after administration and evaluated with fluorescent confocal microscopy.

The liver and spleen were the main targets of Ret NPs. Positive Cy5 uptake and mCherry transfection were found in the cirrhotic liver and both co-localized close to fibrotic tracts (Fig. 2A). In addition, the spleen displayed generalized Cy5 and mCherry positivity. Some Cy5 was also detected in the kidney, but no efficient transfection was observed (Supplementary Figure 1). Importantly, NPs were not uptaken in the lung, heart, or brain. Furthermore, no signal was detected in the main circulatory arteries (Supplementary Figure 2) including the mesenteric artery (Fig. 2A). Finally, the specific hepatic targeting of pBAE NPs was not observed when Ret was absent from the construct (Fig. 2B). Therefore, hepatic targeting selectivity was strongly associated with the presence of the Ret moiety in the construct.

3.3. Liver-targeted NO donor NPs significantly ameliorate PP, without affecting systemic hemodynamics

To evaluate the systemic and portal hemodynamic effects of the NO donor, cirrhotic rats with ascites were intravenously given CT (n = 5) or NO (n = 9) Ret donor Ret pBAE NPs. Both groups showed a similar body weight and amount of ascites (Table 1) and MAP, CO and TPR- in basal conditions. None of these parameters displayed significant changes after the administration of NO donor Ret pBAE NPs. Grey areas are values in
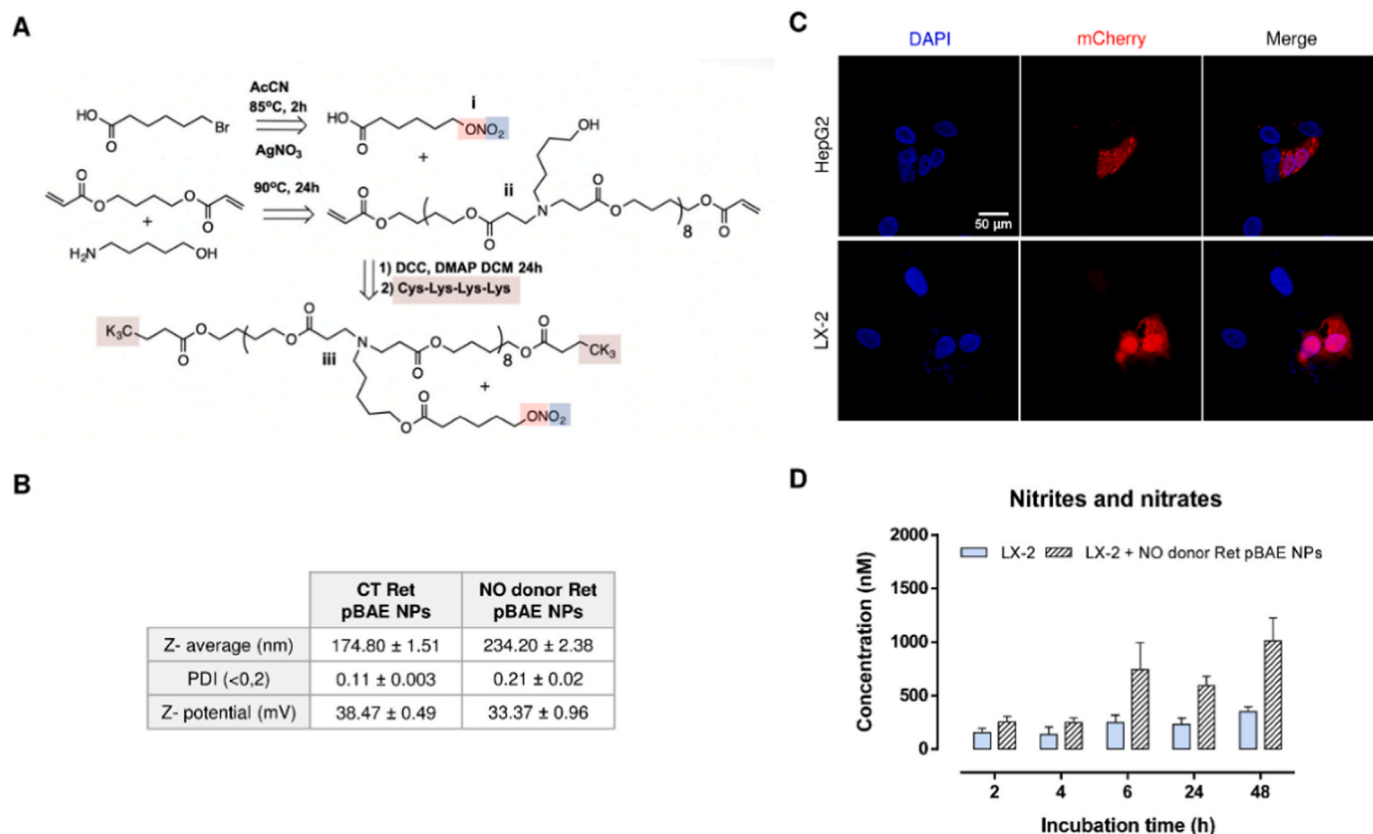
Fig. 1. Synthesis and characterization of Ret pBAE NPs. (A) Chemical reactions to generate a pBAE containing an organic nitrate group: from halide organic acids to its induction through a Steglich esterification reaction using side chain hydroxyls. (B) Z-average hydrodynamic diameter (nm), PDI and Z-potential (mV) measured using dynamic light scattering. (C) Representative fluorescence images (40x) of HepG2 and LX-2 cells treated with mCherry Ret pBAE NPs (1 μg/mL) for 48 h. (D) Quantification of nitrites and nitrates released into the medium by non-treated LX-2 and NO donor Ret pBAE NPs (1 μg/mL) LX-2 treated cells. Results are given as mean ± S.E.

healthy animals treated (n = 5) and non-treated (n = 5) with NO donor Ret pBAE NPs under identical experimental conditions (Fig. 3A). Of note, cirrhotic rats receiving the NO donor showed significantly lower PP in comparison to those receiving CT NPs (Fig. 3B). This occurred in the absence of significant differences in SPP. Both groups of CCl4-treated rats also displayed the characteristic serum biochemistry alteration of cirrhosis including increased levels of transaminases, bilirubin and decreased total proteins and albumin compared to healthy animals. No differences in these parameters were found between healthy animals treated (n = 5) or non-treated (n = 5) with NO donor RetpBAE NPs (data not shown). However, cirrhotic animals treated with liver-targeted NO donor NPs showed a reduction of around 50% in aspartate transaminase and lactate dehydrogenase serum levels compared to cirrhotic rats not receiving NO donor NPs (Table 1). No significant differences were found in bilirubin levels between cirrhotic rats receiving and not receiving the NO donor.

Further knowledge of the hepatic effect of the liver-targeted NO donor was gained using a commercially available PCR array. Only genes with ± 1.5-fold change in hepatic expression and a p < 0.05 were considered biologically and statistically significant (Fig. 3C). Actually, 4 genes were both biologically and significantly downregulated including: bradykinin B1, angiotensin converting enzyme 2, prostaglandin-endoperoxide synthase 2 (*Ptgs2*) and sphingosine kinase 1. *Bradykinin B1* encodes an inducible G-protein-coupled receptor that promotes tissue inflammation [12]. *Angiotensin converting enzyme 2* is an enzyme that catalyzes the conversion of angiotensin II to Ang-(1−7) leading to vasodilation and inhibition of cell proliferation [13]. *Ptgs2* encodes for the protein cyclooxygenase 2, an inducible enzyme involved in the production of prostaglandins [14]. *Sphingosine kinase 1* catalyzes the

phosphorylation of sphingosine inducing inflammation, proliferation, and apoptosis inhibition [15].

3.4. Liver-targeted NO donor NPs reduced liver fibrosis, steatosis, and hepatic stellate cells (HSC) activation

Sirius red staining showed that all cirrhotic rats had perisinusoidal and bridging fibrosis with portal-to-portal septa surrounding the liver nodules. Animals receiving the NO donor showed slightly, albeit significantly, fewer collagen fibers than those given CT NPs (Fig. 4A). Administration of NO donor Ret pBAE NPs to cirrhotic animals was also associated with a moderate but significant decrease in hepatic staining of alpha smooth muscle actin (αSMA) compared to CT NPs (Fig. 4A). Furthermore, most Ret pBAE NPs colocalized with αSMA staining in the cirrhotic liver (Fig. 4B). We also found a marked reduction in liver steatosis following the administration of NO donor Ret pBAE NPs. Indeed, the NO donor decreased lipid droplets (LD) by around 50%, and LD size and count were also reduced as compared CT NPs (38.97 ± 2.4 μm^2 vs 71.45 ± 6 μm^2, p < 0.001 and 576 ± 27 LD/slice vs 831 ± 48 LD/slice, p < 0.001, respectively).

3.5. Hepatic amino acid (AA) concentrations in cirrhotic rats with ascites treated with liver-targeted NO donor polyplexes

In agreement with previous investigations performed in serum [16, 17], the abundance of essential AA was markedly altered in cirrhotic rats with ascites compared to control animals (Supplementary Table 1). The most intense differences were shown by 4-hydroxyproline, aminoadipic acid, arginine, asparagine, aspartic acid, cystine, glutamic acid, glycine,

A

B
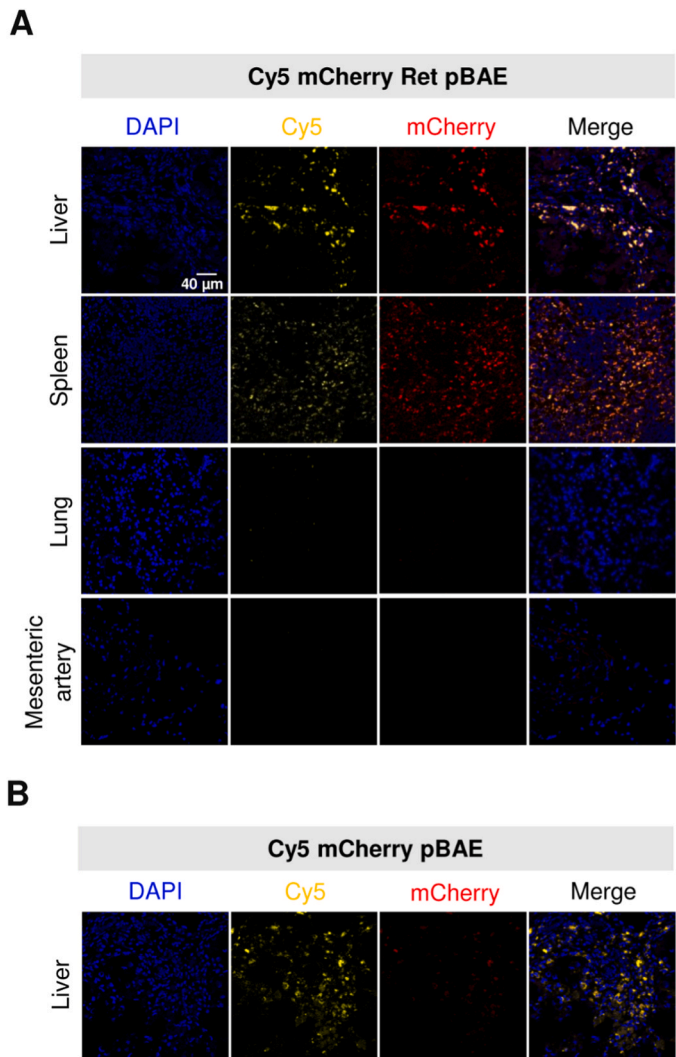
Fig. 2. Tissue biodistribution of Cy5 mCherry Ret pBAE NPs. Representative confocal microscopy fluorescence images at 40x of: (A) liver, spleen, lung and mesenteric artery collected 3 h after Cy5 mCherry Ret pBAE NPs administration to cirrhotic rats. (B) Liver 3 h after the administration of the Cy5 mCherry pBAE NPs without the Ret moiety. Nuclei are stained in blue with DAPI.

phosphoethanolamine, saccharopine, and tyrosine. Furthermore, the administration of NO donor Ret pBAE NP significantly reduced the liver content of the fibrosis marker 4-hydroxyproline by around 30%, in addition to aminoadipic acid and saccharopine (Fig. 5).

3.6. Effects on the expression of genes related to extracellular matrix (ECM) remodeling, vasoactive activity, and growth factors

Assessment of the mRNA expression of a panel of fibrosis-related genes was consistent with almost no effect of NO donor Ret pBAE NPs on transcriptional regulation of ECM. Apart from tissue inhibitor of metalloproteinases (*Timp1*), no differences in gene expression were found between cirrhotic rats receiving or not the NO donor (Supplementary Table 2). *Timp1* is a glycoprotein that regulates of metalloproteinase activity [18]. Additionally, *Timp1* has been involved in apoptosis regulation [19]. Similarly, no differences were observed in the expression of genes involved in cell proliferation and angiogenesis: platelet derived growth factor receptor beta and vascular endothelial growth factor A. By contrast, we did observe a significant reduction in endothelin 1 (*Et-1*), one of the most potent endogenous vasoconstrictors

Table 1
Body weight, ascites volume and serum markers of liver function in control (n = 5) and cirrhotic rats treated with CT (n = 5) or NO donor (n = 9) Ret pBAE NPs.

	Control rats	Cirrhotic rats with ascites	
		CT Ret NPs	**NO donor Ret NPs**
Body weight (g)	407 ± 5.57	406.2 ± 9.37	420.7 ± 19.1
Ascites (mL)	0 ± 0	6.8 ± 2.15 *	9.22 ± 3.07 *
Alanine transaminase (U/L)	41 ± 1.42	282.7 ± 67.45 * *	191.6 ± 39.46 *
Aspartate transaminase (U/L)	94.54 ± 4.81	1384 ± 256.2 * *	671.5 ± 165.2 *,#
Gamma-glutamyl transferase (U/L)	0 ± 0	12.76 ± 1.58 * **	7.64 ± 2.27 *
Lactate dehydrogenase (U/L)	636.3 ± 33.63	2782 ± 418.2 * **	1101 ± 134 *, ###
Total bilirubin (mg/dL)	0 ± 0	1.62 ± 0.43 * *	1.84 ± 0.52 *
Total proteins (g/L)	59.58 ± 0.46	40.66 ± 2.42 * **	39.47 ± 3.13 * **
Albumin (g/L)	33.38 ± 0.46	21.76 ± 1.51 * **	23.71 ± 1.54 * **
Triglycerides (mg/dL)	111.9 ± 22.11	110.2 ± 9.23	80.11 ± 12.53
Total cholesterol (mg/dL)	53.42 ± 3.61	59.5 ± 4.78	58.29 ± 5.80
Glucose (mg/dL)	151.9 ± 6.24	68.55 ± 16.89 * *	73.52 ± 13.57 * *
Creatinine (mg/dL)	0.39 ± 0.01	0.63 ± 0.05 * *	0.57 ± 0.07

$*p < 0.05$, $*p < 0.005$, $* **p < 0.001$ versus control rats and $^{\#}p < 0.05$, $^{\#\#\#}p < 0.001$ CT Ret NPs treated rats. Unpaired Student t-test. Results are given as means ± S.E.

[20].

3.7. Effect of liver-targeted NO donor NPs on hepatic apoptosis and inflammatory mediators

The terminal deoxynucleotidyl transferase dUTP nick-end labeling assay showed a significant decrease in apoptotic DNA fragmentation positive cells in the liver of NO donor-treated cirrhotic rats (Fig. 6A). We also observed a significant decrease of activated caspase-3 (Fig. 6B). These results indicate that treatment with liver-specific NO donor polyplexes decreased cell death. On the other hand, both groups of cirrhotic animals had similar degrees of macrophage infiltrate (Fig. 6C). However, the analysis of messenger expression of a panel of mediators related to macrophage phenotype revealed a significant downregulation in proinflammatory markers, including nitric oxide synthase 2 (*Nos2*), *Ptgs2*, tumor necrosis factor alpha (*Tnfα*), and interleukin 6 (*Il6*) (Fig. 6D) but not in M2-like genes (Fig. 6E).

3.8. Ret pBAE NPs effectively transfect hPCLS of cirrhotic patients

Finally, to determine the ability of Ret pBAE NPs to transfect human cirrhotic tissue, hPCLS were treated with mCherry Ret pBAE NPs for 48 h. The ATP assay showed that the metabolic activity of hPCLS was within the normal limits after 48 h in culture (Fig. 7A). In addition, the efficacy of our construct in the human liver was demonstrated by effective transfection of mcherry Ret NPs in hPCLS (Fig. 7B).

4. Discussion

Patients with portal hypertension have an elevated risk of mortality mainly due to the secondary effects resulting from this condition. The current investigation was addressed to design and evaluate the therapeutic potential of a nanoformulation containing an NO donor selectively aimed at the liver. The main purpose of this strategy was to decrease portal hypertension without affecting the general circulation, thus avoiding the unwanted systemic hemodynamic effects that could
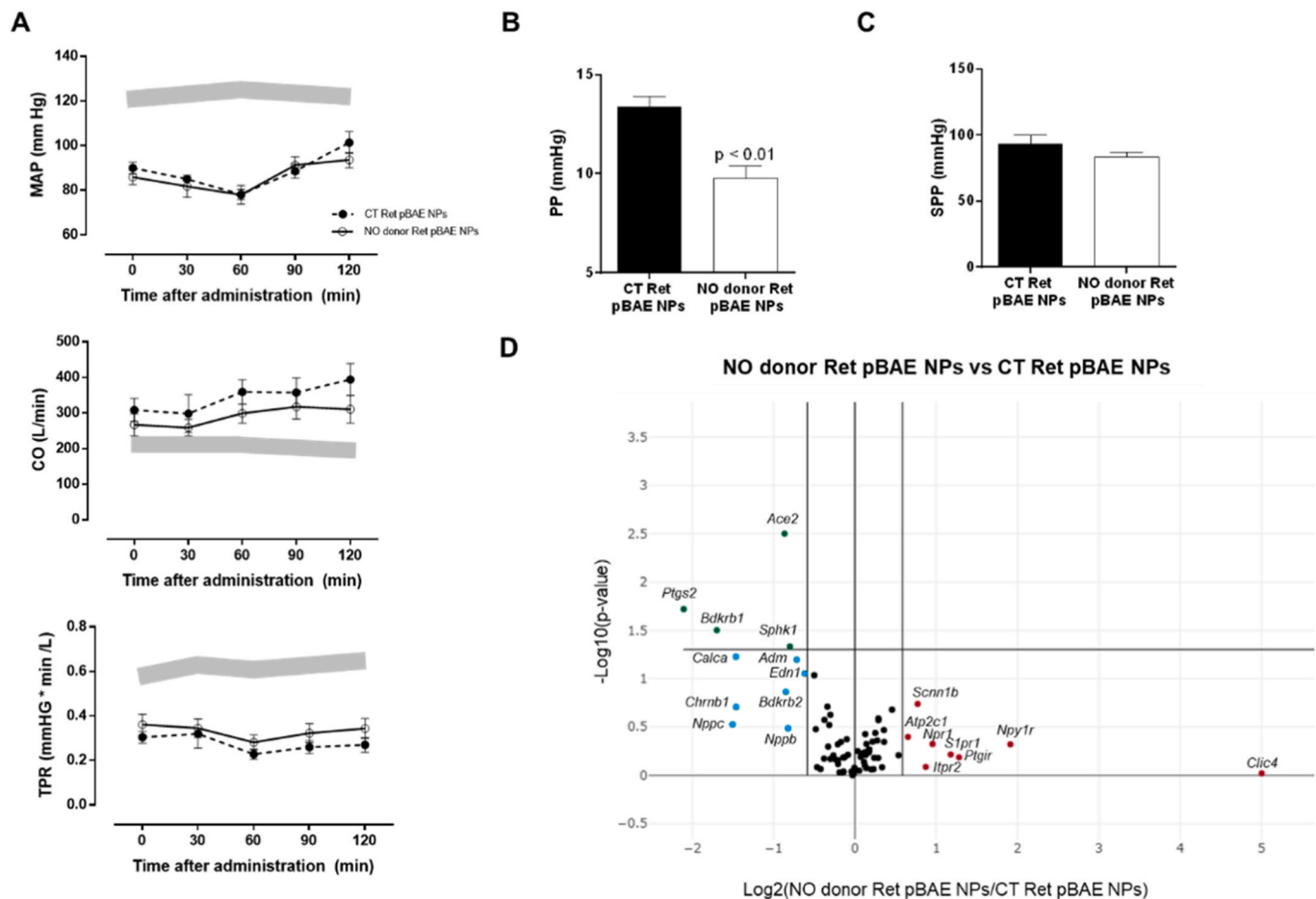
Fig. 3. Effects of liver-targeted NO donor on hemodynamics. Cirrhotic Rats treated with CT (n = 5) or NO donor Ret pBAE NPs (n = 9). (A) MAP, CO and TPR. Grey areas represent values in healthy animals under identical experimental conditions. (B) PP and (C) SPP at the end of the study. Unpaired Student *t*-test. Results are given as mean ± S.E. (D) Volcano plot of differentially expressed genes related to hypertension in a pair-wise comparison. Biological cut-off at ± 1.5-fold change, and significance < 0.05 (Student *t*-test). Insignificant (black), biologically downregulated (blue), upregulated (red), and biologically and statistically significant downregulated (green) in NO donor-treated cirrhotic rats. Abbreviations: bradykinin B1 (*Bdkrb1*), angiotensin converting enzyme 2 (*Ace2*), prostaglandin-endoperoxide synthase 2 (*Ptgs2,*) and sphingosine kinase 1 (*Sphk1*).

result from untargeted systemic administration of this agent.

NO donors are a family of compounds with different chemical groups and pharmacokinetic and dynamic properties specifically designed to release NO or NO-related species [6]. Although displaying positive outcomes in experimental fibrosis/cirrhosis, to date none of these compounds has proven to be effective in any clinical trial, in part due to their non-specific in vivo distribution [5,21].

Here we selected organic nitrates as NO donors because they have excellent stability, and NO release is mediated by the activity of different enzymes, including cytochrome P450 reductase and glutathione S-transferase or by the reaction with thiols from cysteine and cysteine derivatives [22,23].

pBAE are a family of biocompatible and biodegradable polymers synthesized by the Michael addition from an acrylate to a primary amine [24]. pBAE are cationic polymers, that are easy to synthetize, and are valuable for their tunable physicochemical properties [25]. They can include functional groups, drugs and/or targeting moieties covalently attached to their structure [26,27]. To form NPs, the addition of genetic material is essential to achieve the electrostatic interaction with the polymer [28].

We first evaluated whether our Ret decorated pBAE NPs were able to in vitro target human-derived liver cells. Fluorescence microscopy of HepG2 and LX-2 cell lines incubated with mCherry Ret pBAE NPs showed mCherry plasmid transfection, supporting the feasibility of using this construct in humans. This was further supported on loading

LX-2 cells with NO donor Ret pBAE NPs, since the conditioned media of these cells showed higher concentrations of nitrites and nitrates than LX-2 cells loaded with Ret pBAE NPs.

As discussed above, the suitability of NO donor Ret pBAE NPs for portal hypertension is largely dependent on their preferential accumulation in the liver. Most Ret pBAE NPs were detected in the liver and spleen of cirrhotic rats. However, marked differences in the signal pattern was noted. Whereas Cy5 and mCherry signals did not show a particular location in the spleen, they displayed a preferential distribution close to the fiber-like zones in the liver. Some NPs were also found in the kidney, but no efficient transfection was detected. In decompensated liver disease, selectivity for the liver is of special importance to prevent potential off-target effects and no further aggravation of systemic vasodilation and arterial hypotension. For this reason, Cy5 and mCherry derived fluorescence was also evaluated in the major systemic vessels. No fluorescent signal was detected in any of these vessels, supporting the hepatic-specificity of the NPs.

A major goal of the current investigation was to develop a therapeutic system that reduces PP without affecting MAP. In cirrhosis, portal hypertension may lead to bleeding, a life-threatening complication that is the cause of death in about one third of the patients [29]. Nonselective β-blockers have been used for decades to treat portal hypertension; however, their efficiency is suboptimal since there is growing evidence suggesting that their indication may be controversial in patients with end-stage liver disease [29,30]. Therefore, novel therapies aimed at
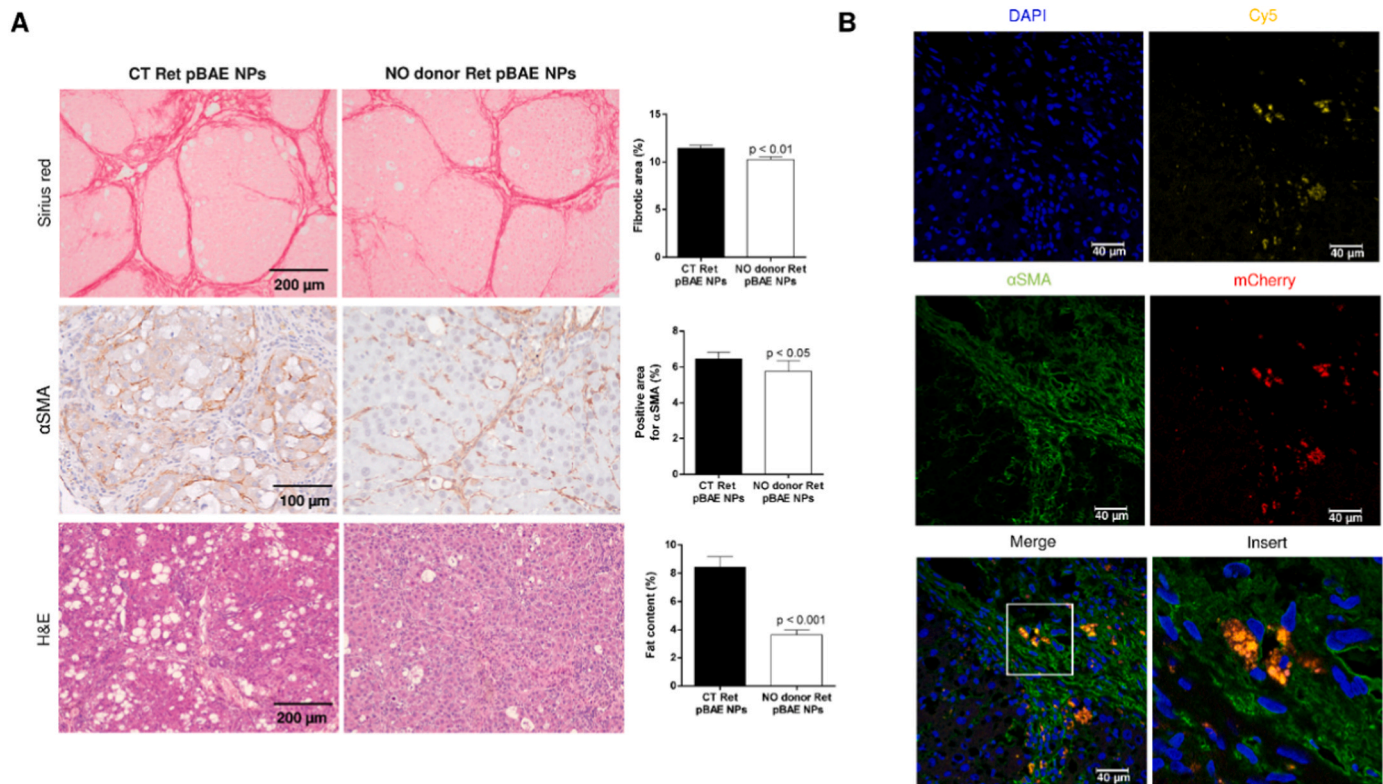
Fig. 4. Effects of liver-targeted NO donor on collagen fibers and steatosis. Cirrhotic rats treated with CT (n = 5) or NO donor Ret pBAE NPs (n = 9). (A) Representative images and morphometric quantification of Sirius red (100x), αSMA (200x) and steatosis (hematoxylin and eosin, H&E, 200x) staining in liver sections. Mann-Whitney test. Results are given as mean ± S.E. (B) Representative confocal fluorescence images of liver biopsies colocalizing Cy5 mCherry Ret pBAE NPs and αSMA-Alexa 488 staining (40x).

reducing PP within a short period of time in patients with cirrhosis are needed. In this investigation, the administration of the liver-targeted NO donor resulted in an average 30% reduction in PP within two hours. It has been reported that a 20% reduction in PP significantly reduces the incidence of variceal bleeding, which is a life-threatening condition for cirrhotic patients [31]. In addition, this did not result in alterations in MAP, CO or TPR. Although some Ret NPs also transfected the spleen, no effect was found in SPP calculation, suggesting that the treatment did not result in non-targeted vasodilation. A reduction in PP was indeed associated with reduced expression of genes involved in inflammation and blood pressure regulation, and serum concentrations of unspecific markers of liver injury including aspartate transaminase and lactate dehydrogenase. This would be an additional indication that beyond its effects on PP, the NO donor also has beneficial consequences in liver damage. All these results strongly support the safety and efficacy of NO donor Ret pBAE NPs treatment at the preclinical level.

Previous studies using liver-targeted and untargeted NO donors have already demonstrated that long term NO administration decreases hepatic fibrogenesis [32–34]. We obtained clear evidence that our NO donor Ret pBAE NPs attenuate liver fibrogenesis in cirrhotic rats. In fact, the liver-targeted NO donor induced a decrease in hepatic Sirius red and αSMA staining, as well hydroxyproline concentrations, a widely accepted biomarker of liver fibrosis [35], in cirrhotic rats compared to CT NPs. Moreover, the high specificity of the NO donor Ret pBAE NPs for the HSCs is a likely explanation for their efficacy to improve the liver architecture.

Cirrhotic rats with ascites also showed an alteration in the concentration of other AA compared to control rats. Several authors have previously described an alteration of aromatic and branched-chain AAs in serum of patients and experimental models with liver disease [16,17, 36]. Similar results were obtained in the present work, revealing an increase of methionine, serine, proline, and aromatic AAs

(phenylalanine, tyrosine and tryptophan) in cirrhotic rats compared to control animals. However, an increase of branched-chain AAs in the cirrhotic liver was observed contrarily to previously reported results in serum. Finally, NO donor treatment resulted in a significant decrease of aminoadipic acid and saccharopine content, both intermediates of lysine catabolism [37]. Elevated serum aminoadipic acid has been associated with adipogenesis and insulin resistance [38]. Moreover, we found a marked reduction of *Et-1* mRNA expression following NO donor administration. ET-1 is a powerful endothelium-derived vasoconstrictor peptide that has shown to be increased in the cirrhotic liver [20] and is thought to be a major player in the pathogenesis of portal hypertension [39]. The inhibitory effect of NO on ET-1 expression and its concomitant vascular vasodilation has previously been demonstrated in several pathological conditions [40] and could be one of the mechanisms mediating the portal vasodilator effect induced by the liver-targeted NO donor.

Several studies have demonstrated the feasibility of adding different targeting moieties to the pBAE polyplexes to target hepatic cancer cells [41,42]. We selected Ret as the hepatic-targeting moiety given that the liver is the most important storage site for retinoids in the body [43]. We have previously shown that adding Ret to end-oligopeptide modified pBAE NPs improved hepatic accumulation after i.v. administration to healthy mice [9]. In the present study, we further demonstrate that NO donor Ret pBAE NPs mainly target HSCs, located close to the fibrotic septa. This fully coincides with previous studies performed in bile-duct ligated rats showing that HSCs actively take up and store Ret, a phenomenon mediated by Ret interaction with Ret receptors for the Ret binding protein [32]. The specificity of the NO donor Ret pBAE NPs for HSCs provides the rationale to explain the effect, other than intrahepatic vasodilation, induced by these polyplexes in the liver of cirrhotic rats.

Changes in the hepatic architecture induced by the administration of the NO donor also affected liver steatosis. In fact, although no
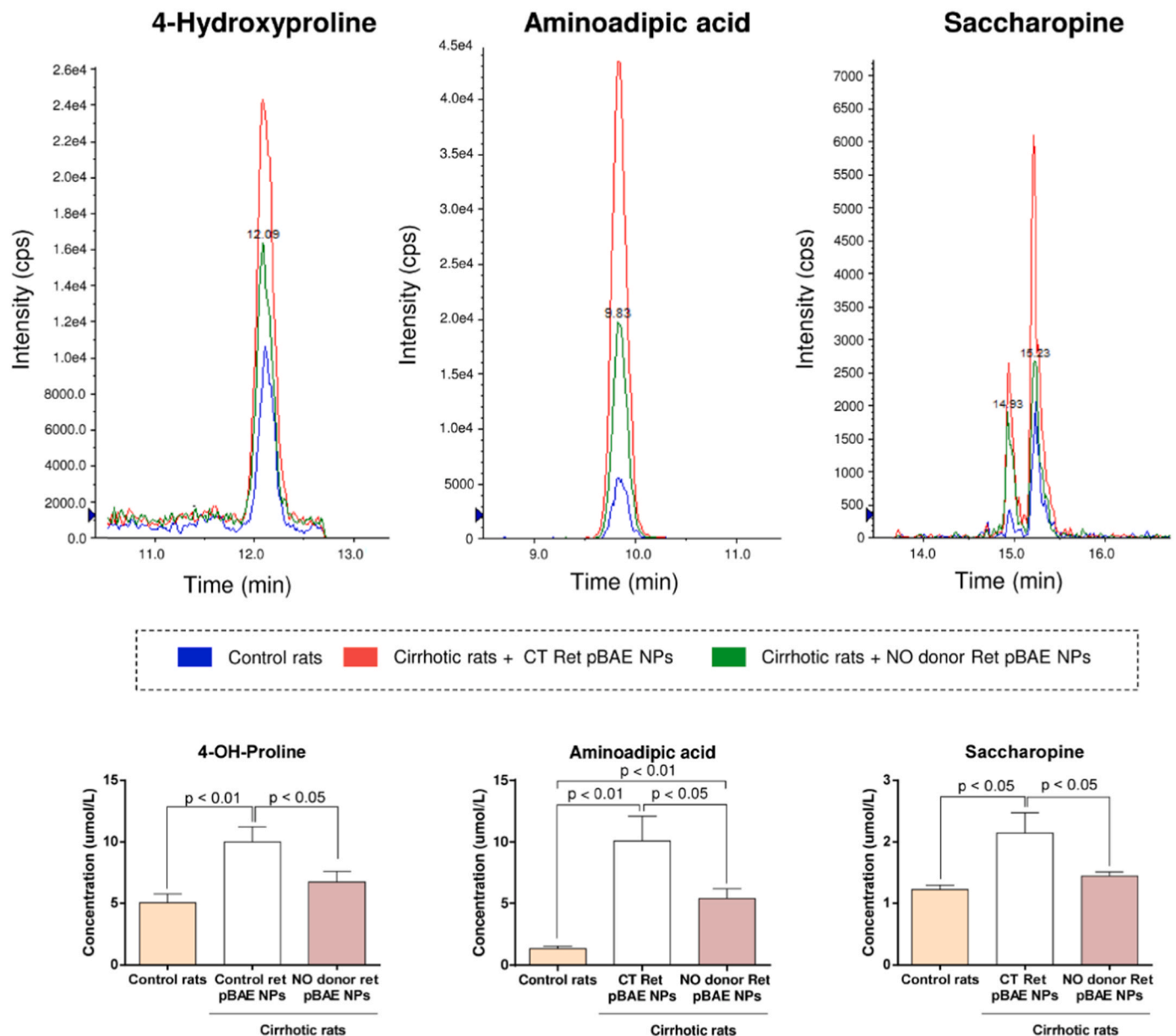
Fig. 5. The effect of liver-specific NO on hepatic AA concentrations in control rats and rats with decompensated cirrhosis. Representative UPLC-MS/MS chromatograms and quantification graphs of significantly reduced AA following administration of NO donor Ret pBAE NPs to cirrhotic rats. Unpaired Student *t*-test or Mann-Whitney test when appropriate. Results are given as mean ± S.E.

differences in serum triglycerides and total cholesterol were observed between animals receiving and not receiving the NO donor, the NO donor decreased hepatic fat content and LD size in cirrhotic rats. This apparently contradictory result may be at first explained by the fact that two hours following NO donor administration the intensity of steatosis is still quite high and the significant steatosis reduction promoted by NPs containing the NO donor is not sufficient to translate into a change in serum lipids.

Further evidence supporting the modulatory effect of the NO donor on the liver architecture of cirrhotic rats was strengthened by the reduction in apoptotic activity. According to the cell type, NO may promote or inhibit apoptosis [44]. In hepatocytes NO behaves as an apoptosis inhibitor by decreasing the activity of mediators of cell death, such as caspases and proteases. In this regard, the hepatoprotective effect of the NO donor in our cirrhotic rats was associated with approximately a 50% reduction in caspase-3 abundance. This is consistent with the previous investigation by T.R. Billiar's laboratory demonstrating that

inhibition of apoptosis by NO is secondary to suppression of caspase-3 like activity by means of mechanisms dependent on cyclic guanosine monophosphate [45].

The effects of the NO donor on liver inflammatory response were more controversial. The liver-specific NO donor did not modify liver inflammatory infiltrate or messenger expression of genes mediating M2 response, however it induced a reduction of mRNA expression of proinflammatory genes. *Ptgs2* modulates inflammation, apoptosis, and cell senescence [46]. Additionally, it has been reported that NO is able to inhibit nuclear factor kappa beta activation [47], a master regulator of innate and adaptive immunities [48]. In agreement, the expression of the proinflammatory cytokines *Il6* and *Tnfα* along with *Nos2*, was decreased in the liver of NO donor treated cirrhotic rats.

A human preclinical demonstration that Ret pBAE NPs may also target and transfect hepatic human cells was obtained using hPCLS. The limitations of animal models to study diseases and the potential effects of treatments are well known. hPCLS are tissue explants that can be
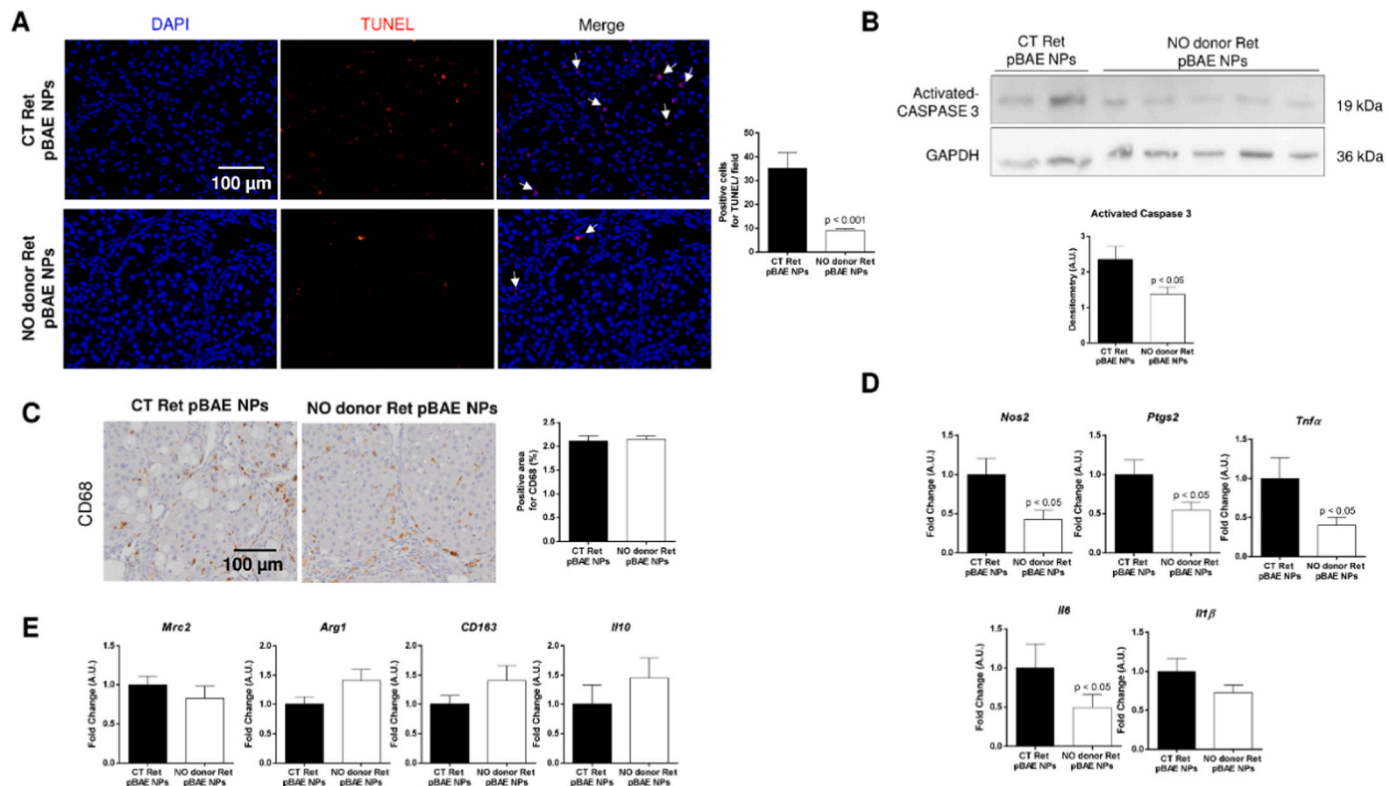
Fig. 6. Effects of liver-targeted NO donor on hepatic apoptosis and inflammation. (A) Representative TUNEL assay in liver sections (200x). White arrows point to apoptotic (red) cells. Bars show the quantification of TUNEL-positive cells/field. (B) Representative western blot for activated caspase-3 in liver tissue. (C) Representative CD68 stained liver sections (200x). The graph shows the morphometric measurement. (D) Hepatic mRNA expression of a panel of proinflammatory markers. (E) Hepatic mRNA expression of M2-like markers. Unpaired Student *t*-test or Mann-Whitney test when appropriate. Results are given as mean ± S.E. Abbreviations: Arg1, arginase 1; CD163, cluster of differentiation 163; GAPDH, glyceraldehyde 3-phosphate dehydrogenase; Il, interleukin; Mrc2, mannose receptor C type 2; Nos2, nitric oxide synthase 2; Ptgs2, prostaglandin endoperoxide synthase 2; Tnfa, tumor necrosis factor alpha.
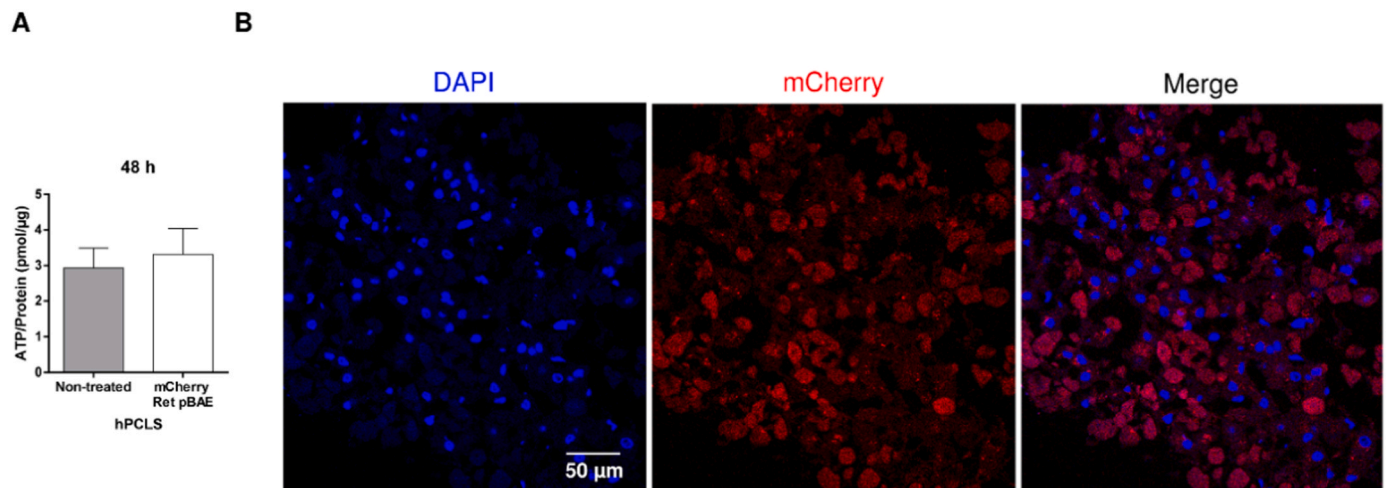
Fig. 7. Transfection of mCherry Ret pBAE NPs in hPCLS. (A) ATP/protein ration measured in hPCLS. (B) Representative confocal microscopy fluorescence images at 40x after 48 h of incubation with mCherry Ret pBAE NPs. Nuclei are stained in blue with DAPI.

cultured ex vivo and closely recapitulate the anatomical architecture, multicellular characteristics, and some functions of the human organ [49]. They represent a valuable tool to provide further information on the possible effects of new treatments in humans. In this regard, our results showing transfection of the Ret pBAE NPs in human tissue parallel previous investigations using hPCLS to evaluate the potential effect of antifibrotic drugs [50], gene therapy [51] and nanoformulations [52] in humans.

In summary, our findings suggest that NO donor Ret pBAE NPs are avidly and specifically internalized by the liver after i.v. administration. Liver cells, mainly HSCs, induce the release of NO from the polyplexes resulting in intrahepatic vasodilation, ultimately leading to decreased portal hypertension and the reduction of inflammatory markers. These results suggest that liver-targeted NO donor pBAE NPs could be of therapeutic value in attenuating portal hypertension and hepatic inflammation in patients with decompensated liver disease.

5. Conclusions

The present study proposes a novel therapeutic approach for portal hypertension based on liver-targeted pBAE NPs containing a NO donor. The addition of Ret as the targeting moiety specifically induced the uptake and transfection of the NPs by hepatic cells. It was demonstrated that when administered i.v. NO donor Ret pBAE NPs significantly decrease portal hypertension without affecting MAP or CO in cirrhotic rats with ascites. Moreover, the hepatic targeted NO donor pBAE NPs significantly diminished HSC activation, hepatic fibrogenesis, steatosis and the expression of proinflammatory gene markers. Finally, these NPs also transfected hPCLS. The current work provides a new approach to improve intrahepatic NO delivery in experimental decompensated cirrhosis.

CRediT authorship contribution statement

Melgar-Lesmes Pedro: Writing – review & editing, Funding acquisition. **Morales-Ruiz Manuel:** Writing – review & editing, Resources, Investigation. **García-Villoria Judith:** Writing – review & editing, Resources, Investigation. **Fornaguera Cristina:** Writing – review & editing, Supervision, Methodology. **Moreno-Lanceta Alazne:** Writing – review & editing, Methodology, Investigation. **Fernández-Varo Guillermo:** Writing – review & editing, Supervision, Methodology, Investigation, Conceptualization. **Jiménez Wladimiro:** Writing – original draft, Visualization, Validation, Supervision, Resources, Project administration, Methodology, Funding acquisition, Formal analysis, Data curation, Conceptualization. **Navalón-López María:** Writing – review & editing, Methodology, Investigation. **Borrós Salvador:** Writing – review & editing, Supervision, Resources, Project administration, Funding acquisition, Conceptualization. **Perramón Meritxell:** Writing – original draft, Visualization, Validation, Methodology, Investigation, Formal analysis, Conceptualization. **López-Moya Mario:** Resources, Methodology. **Faneca Joana:** Writing – review & editing, Investigation. **García-Pérez Rocío:** Writing – review & editing, Resources.

Declaration of Competing Interest

The authors declare that they have no known competing financial interests or personal relationships that could have appeared to influence the work reported in this paper.

Acknowledgments

We thank D.Pringle for language and style review.

Appendix A. Supporting information

Supplementary data associated with this article can be found in the online version at doi:10.1016/j.biopha.2024.116143.

References

[1] L.S. Hu, J. George, J.H. Wang, Current concepts on the role of nitric oxide in portal hypertension, World J. Gastroenterol. 19 (11) (2013) 1707–1717, https://doi.org/10.3748/wjg.v19.i11.1707.

[2] D.A. Simonetto, M. Liu, P.S. Kamath, Portal hypertension and related complications: diagnosis and management, Mayo Clin. Proc. 94 (4) (2019) 714–726, https://doi.org/10.1016/j.mayocp.2018.12.020.

[3] S. Moller, J. Henriksen, Ascites and Renal Dysfunction in Liver Disease: Pathogenesis, in: P. Ginès, V. Arroyo, J. Rodés, R. Schrier (Eds.), Diagnosis, and Treatment, Vol. 1, Wiley-Blackwell, New Jersey, USA, 2005.

[4] M. Morales-Ruiz, P. Cejudo-Martín, G. Fernández-Varo, S. Tugues, J. Ros, P. Angeli, et al., Transduction of the liver with activated Akt normalizes portal pressure in cirrhotic rats, Gastroenterology 125 (2) (2003) 522–531, https://doi.org/10.1016/s0016-5085(03)00909-0.

[5] A. Berzigotti, P. Bellot, A. De Gottardi, J.C. Garcia-Pagan, C. Gagnon, J. Spénard, J. Bosch, NCX-1000, a nitric oxide-releasing derivative of UDCA, does not decrease portal pressure in patients with cirrhosis: results of a randomized, double-blind, dose-escalating study, Am. J. Gastroenterol. 105 (5) (2010) 1094–1101, https://doi.org/10.1038/ajg.2009.661.

[6] R. Scateana, P. Bottoni, A. Pontoglio, B. Giardina, Pharmacological modulation of nitric oxide release: new pharmacological perspectives, potential benefits and risks, Curr. Med Chem. 17 (1) (2010) 61–73, https://doi.org/10.2174/092986710789957841.

[7] Y. Iwakiri, Y. Kim, MY. Nitric oxide in liver diseases, Trends Pharm. Sci. 36 (8) (2015) 524–536, https://doi.org/10.1016/j.tips.2015.05.001.

[8] C.E. Carnovale, M.T. Ronco, Role of nitric oxide in liver regeneration, Ann. Hepatol. 11 (5) (2012) 636–647, https://doi.org/10.1016/S1665-2681(19)31436-X.

[9] C. Fornaguera, M. Guerra-Rebollo, M.Á. Lázaro, A. Cascante, N. Rubio, J. Blanco, et al., In vivo retargeting of poly(beta aminoester) (OM-PBAE) nanoparticles is influenced by protein corona, Adv. Health Mater. 8 (19) (2019) e1900849, https://doi.org/10.1002/adhm.201900849.

[10] J. Clària, W. Jiménez, Experimental Models of Cirrhosis and Ascites in Ascites and Renal Dysfunction in Liver Disease: Pathogenesis Diagnosis and Treatment, in: P. Ginès, V. Arroyo, J. Rodés, R. Schrier (Eds.), Ch, Vol. 1, Wiley-Blackwell, New Jersey, USA, 2005, pp. 215–226.

[11] R. Wijngaard, M. Perramón, M. Parra-Robert, S. Hidalgo, G. Butrico, M. Morales-Ruiz, et al., Validation of a gas chromatography-mass spectrometry method for the measurement of the redox state metabolic ratios lactate/pyruvate and β-hydroxybutyrate/acetoacetate in biological samples, Int J. Mol. Sci. 22 (9) (2021) 4752, https://doi.org/10.3390/ijms22094752.

[12] W.E. Stansfield, M. Ranek, A. Pendse, J.C. Schisler, S. Wang, T. Pulinilkunnil, et al., The pathophysiology of cardiac hypertrophy and heart failure, Chapter 4. Cellular and Molecular Pathobiology of Cardiovascular Disease, Academic Press, 2014, pp. 51–78. Chapter 4.

[13] C.B. Herath, F.J. Warner, J.S. Lubel, R.G. Dean, Z. Jia, R.A. Lew, et al., Upregulation of hepatic angiotensin-converting enzyme 2 (ACE2) and angiotensin-(1–7) levels in experimental biliary fibrosis, J. Hepatol. 47 (3) (2007) 387–395, https://doi.org/10.1016/j.jhep.2007.03.008.

[14] E. Ricciotti, G.A. FitzGerald, Prostaglandins and inflammation, Arterioscler. Thromb. Vasc. Biol. 31 (5) (2011) 986–1000, https://doi.org/10.1161/ATVBAHA.110.207449.

[15] H. Alshaker, L. Sauer, D. Monteil, S. Ottaviani, S. Srivats, T. Böhler, et al., Therapeutic potential of targeting SK1 in human cancers, Adv. Cancer Res 117 (2013) 143–200, https://doi.org/10.1016/B978-0-12-394274-6.00006-6.

[16] L. Fontana, E. Moreira, M.I. Torres, M.I. Fernández, A. Ríos, S.ánchez de Medina, F. Gil, A. Serum amino acid changes in rats with thioacetamide-induced liver cirrhosis, Toxicology 106 (1-3) (1996) 197–206, https://doi.org/10.1016/0300-483x(95)03177-h.

[17] M. Holeček, M. Mráz, J. Tilšer, I. Plasma amino acids in four models of experimental liver injury in rats, Amino Acids 10 (3) (1996) 229–241, https://doi.org/10.1007/BF00807325.

[18] N.D. Thiele, J.W. Wirth, D. Steins, A.C. Koop, H. Ittrich, A.W. Lohse, et al., TIMP-1 is upregulated, but not essential in hepatic fibrogenesis and carcinogenesis in mice, Sci. Rep. 7 (1) (2017) 714, https://doi.org/10.1038/s41598-017-00671-1.

[19] K. Wang, B. Lin, J.J. Brems, R.L. Gamelli, Hepatic apoptosis can modulate liver fibrosis through TIMP1 pathway, Apoptosis 18 (5) (2013) 566–577, https://doi.org/10.1007/s10495-013-0827-5.

[20] A. Leivas, W. Jiménez, J. Bruix, L. Boix, J. Bosch, V. Arroyo, et al., Gene expression of endothelin-1 ET(A) andET(B) receptors in human cirrhosis: relationship with hepatic hemodynamics, J. Vasc. Res 35 (3) (1998) 186–193, https://doi.org/10.1159/000025583.

[21] S. Fiorucci, E. Antonelli, O. Morelli, A. Mencarelli, A. Casini, T. Mello, et al., NCX-1000, a NO-releasing derivative of ursodeoxycholic acid, selectively delivers NO to the liver and protects against development of portal hypertension, Proc. Natl. Acad. Sci. USA 98 (15) (2001) 8897–8902, https://doi.org/10.1073/pnas.151136298.

[22] M.S. França-Silva, C.M. Balarini, J.C. Cruz, B.A. Khan, P.H. Rampelotto, V. A. Braga, Organic nitrates: past, present and future, Molecules 19 (9) (2014) 15314–15323, https://doi.org/10.3390/molecules190915314.

[23] A. Daiber, T. Münzel, Organic nitrate therapy, nitrate tolerance, and nitrate-induced endothelial dysfunction: emphasis on redox biology and oxidative stress, Antioxid. Redox Signal 23 (11) (2015) 899–942, https://doi.org/10.1089/ars.2015.6376.

[24] Y. Liu, Y. Li, D. Keskin, L. Shi, Poly(β-amino esters): synthesis, formulations, and their biomedical applications, Adv. Health Mater. 8 (2) (2019) e1801359, https://doi.org/10.1002/adhm.201801359.

[25] M. Navalón-López, A. Dols-Perez, S. Grijalvo, C. Fornaguera, S. Borrós, Unravelling the role of individual components in pBAE/polynucleotide polyplexes in the synthesis of tailored carriers for specific applications: on the road to rational formulations, Nanoscale Adv. 5 (6) (2023) 1611–1623, https://doi.org/10.1039/d2na00800a.

[26] C. Fornaguera, M. Guerra-Rebollo, M. Ángel Lázaro, C. Castells-Sala, O. Meca-Cortés, V. Ramos-Pérez, et al., mRNA delivery system for targeting antigen-presenting cells in vivo, Adv. Health Mater. 7 (17) (2018) e1800335, https://doi.org/10.1002/adhm.201800335.

[27] P. Dosta, I. Tamargo, V. Ramos, S. Kumar, D.W. Kang, S. Borrós, et al., Delivery of Anti-microRNA-712 to inflamed endothelial cells using Poly(β-amino ester) nanoparticles conjugated with VCAM-1 targeting peptide, Adv. Health Mater. 10 (15) (2021) e2001894, https://doi.org/10.1002/adhm.202001894.

[28] D.M. Lynn, R. Langer, Degradable poly(β-amino esters): synthesis, characterization, and self-assembly with plasmid DNA, J. Am. Chem. Soc. 122 (44) (2000) 10761–10768, https://doi.org/10.1021/ja0015388.

[29] J. Bosch, R.J. Groszmann, V.H. Shah, Evolution in the understanding of the pathophysiological basis of portal hypertension, How Chang. Paradig. Lead. Success. N. Treat. J. Hepatol. 62 (1Suppl) (2015) S121–S130, https://doi.org/10.1016/j.jhep.2015.01.003.

[30] S.G. Rodrigues, Y.P. Mendoza, J. Bosch, Beta-blockers in cirrhosis: evidence based indications and limitations, JHEP Rep. 2 (1) (2019) 100063, https://doi.org/10.1016/j.jhepr.2019.12.001.

[31] G. Garcia-Tsao, A.J. Sanyal, N.D. Grace, W. Carey, Practice guidelines committee of the american association for the study of liver diseases; practice parameters committee of the american college of gastroenterology. Prevention and management of gastroesophageal varices and variceal hemorrhage in cirrhosis, Am. J. Gastroenterol. 102 (9) (2007) 2086–2102.

[32] H.T.T. Duong, Z. Dong, L. Su, C. Boyer, J. George, T.P. Davis, et al., The use of nanoparticles to deliver nitric oxide to hepatic stellate cells for treating liver fibrosis and portal hypertension, Small 11 (19) (2015) 2291–2304, https://doi.org/10.1002/smll.201402870.

[33] F. Moal, N. Veal, E. Vuillemin, E. Barrière, J. Wang, L. Fizanne, et al., Hemodynamic and antifibrotic effects of a selective liver nitric oxide donor VPYRRO/ NO in bile duct ligated rats, World J. Gastroenterol. 12 (41) (2006) 6639–6645, https://doi.org/10.3748/wjg.v12.i41.6639.

[34] J. Sun, M. Li, S. Fan, Z. Guo, B. Zhong, X. Jin, et al., A novel liver-targeted nitric oxide donor UDCA-Thr-NO protects against cirrhosis and portal hypertension, Am. J. Transl. Res 10 (2) (2018) 392–401.

[35] S.A. Gabr, A.H. Alghadir, Y.E. Sherif, A.A. Ghfar, Hydroxyproline as a biomarker in liver disease, in: V. Patel, V. Preedy (Eds.), Biomarkers in Liver Disease. Biomarkers in Disease: Methods, Discoveries and Applications, Springer, Dordrecht, 2017.

[36] J. Zhang, Y. Yang, Z. Wang, X. Zhang, Y. Zhang, J. Lin, et al., Integration of metabolomics, lipidomics, and proteomics reveals the metabolic characterization of nonalcoholic steatohepatitis, J. Proteome Res 22 (8) (2023) 2577–2592, https://doi.org/10.1021/acs.jproteome.3c00009.

[37] P. Arruda, P. Barreto, Lysine catabolism through the saccharopine pathway: enzymes and intermediates involved in plant responses to abiotic and biotic stress, Front Plant Sci. 11 (2020) 587, https://doi.org/10.3389/fpls.2020.00587.

[38] H.J. Lee, H.B. Jang, W. Kim, K.J. Park, K.W. Kim, S.I. Park, et al., 2-Aminoadipic acid (2-AAA) as a potential biomarker for insulin resistance in childhood obesity, Sci. Rep. 9 (1) (2019) 13610, https://doi.org/10.1038/s41598-019-49578-z.

[39] M. Morales-Ruiz, W. Jiménez, Nitric Oxide and Systemic and Renal Hemodynamic Disturbances in Cirrhosis, in: P. Ginès, V. Arroyo, J. Rodés, R. Schrier (Eds.), In Ascites and Renal Dysfunction in Liver Disease: Pathogenesis, Diagnosis, and Treatment, Vol 1, Wiley-Blackwell, New Jersey, USA, 2005.

[40] D.C. Rockey, Endothelial dysfunction in advanced liver disease, Am. J. Med Sci. 349 (1) (2015) 6–16, https://doi.org/10.1097/MAJ.0000000000000403.

[41] C.G. Zamboni, K.L. Kozielski, H.J. Vaughan, M.M. Nakata, J. Kim, L.J. Higgins, et al., Polymeric nanoparticles as cancer-specific DNA delivery vectors to human hepatocellular carcinoma, J. Control Release 263 (2017) 18–28, https://doi.org/10.1016/j.jconrel.2017.03.384.

[42] H.J. Vaughan, C.G. Zamboni, N.P. Radant, P. Bhardwaj, E. Revai Lechtich, L. F. Hassan, et al., Poly(beta-amino ester) nanoparticles enable tumor-specific TRAIL secretion and a bystander effect to treat liver cancer, Mol. Ther. Oncolytics 21 (2021) 377–388, https://doi.org/10.1016/j.omto.2021.04.004.

[43] Y. Shirakami, S.-A. Lee, R.D. Clugston, W.S. Blaner, Hepatic metabolism of retinoids and disease associations, Biochim Biophys. Acta 1821 (1) (2012) 124–136, https://doi.org/10.1016/j.bbalip.2011.06.023.

[44] P.K. Kim, R. Zamora, P. Petrosko, T.R. Billiar, The regulatory role of nitric oxide in apoptosis. 1 (8) (2001) 1421–1441, https://doi.org/10.1016/s1567-5769(01)00088-1.

[45] Y. Kim, Y.M. Talanian, R.V. Billiar, T R. Nitric oxide inhibits apoptosis by preventing increases in caspase-3-like activity via two distinct mechanisms, J. Biol. Chem. 272 (49) (1997) 31138–31148, https://doi.org/10.1074/jbc.272.49.31138.

[46] H. Yang, Y. Xuefeng, W. Shandong, X. Jianhua, COX-2 in liver fibrosis, Clin. Chim. Acta 506 (2020) 196–203, https://doi.org/10.1016/j.cca.2020.03.024.

[47] I.M. Grumbach, W. Chen, S.A. Mertens, D.G. Harrison, A negative feedback mechanism involving nitric oxide and nuclear factor kappa-B modulates endothelial nitric oxide synthase transcription, J. Mol. Cell Cardiol. 39 (4) (2005) 595–603, https://doi.org/10.1016/j.yjmcc.2005.06.012.

[48] T. Liu, L. Zhang, D. Joo, S.-C. Sun, NF-κB signaling in inflammation, Signal Transduct. Target Ther. 2 (1) (2017) 17023, https://doi.org/10.1038/sigtrans.2017.23.

[49] D. Majorova, E. Atkins, H. Martineau, I. Vokra, D. Oosterhuis, P. Olinga, et al., Use of precision-cut tissue slices as a translational model to study host-pathogen interaction, Front Vet. Sci. 8 (2021) 686088, https://doi.org/10.3389/fvets.2021.686088.

[50] I.M. Westra, D. Oosterhuis, G.M. Groothuis, P. Olinga, The effect of antifibrotic drugs in rat precision-cut fibrotic liver slices, PLoS One 9 (4) (2014) e95462, https://doi.org/10.1371/journal.pone.0095462.

[51] M. Ruigrok, M.J.R. Xian, J.L. Frijlink, H.W. Melgert, B.N. Hinrichs, W.J. Olinga, siRNA-mediated protein knockdown in precision-cut lung slices, Eur. J. Pharm. Biopharm. 133 (2018) 339–348, https://doi.org/10.1016/j.ejpb.2018.11.005.

[52] R. Bartucci, C. Åberg, B.N. Melgert, Y.L. Boersma, P. Olinga, A. Salvati, Time-Resolved Quantification of Nanoparticle Uptake, Distribution, and Impact in Precision-Cut Liver Slices, Small 16 (21) (2020) e1906523, https://doi.org/10.1002/smll.201906523.